ALMA MATER STUDIORUM
UNIVERSITÀ DI BOLOGNA

ARCHIVIO ISTITUZIONALE
DELLA RICERCA

Alma Mater Studiorum Università di Bologna
Archivio istituzionale della ricerca

Could hypoxia influence basic biological properties and ultrastructural features of adult canine mesenchymal stem /stromal cells?

This is the final peer-reviewed author’s accepted manuscript (postprint) of the following publication:

Published Version:
Iacono, E., Pascucci, L., Bazzucchi, C., Cunto, M., Ricci, F., Rossi, B., et al. (2018). Could hypoxia influence basic biological properties and ultrastructural features of adult canine mesenchymal stem /stromal cells?. VETERINARY RESEARCH COMMUNICATIONS, 42(4), 297-308 [10.1007/s11259-018-9738-9].

Availability:
This version is available at: https://hdl.handle.net/11585/649006 since: 2019-02-12

Published:
DOI: http://doi.org/10.1007/s11259-018-9738-9

Terms of use:

Some rights reserved. The terms and conditions for the reuse of this version of the manuscript are specified in the publishing policy. For all terms of use and more information see the publisher's website.

This item was downloaded from IRIS Università di Bologna (https://cris.unibo.it/).
When citing, please refer to the published version.

(Article begins on next page)

06 May 2026

"This is a post-peer-review, pre-copyedit version of an article published in Veterinary Research Communications. The final authenticated version is available online at: http://dx.doi.org/10.1007/s11259-018-9738-9.

This version is subjected to Springer Nature terms for reuse that can be found at: https://www.springer.com/gp/open-access/authors-rights/aam-terms-v1

14 **Could hypoxia influence basic biological properties and ultrastructural features of adult**

15 **canine mesenchymal stem /stromal cells?**

16

17 Eleonora Iacono[1]*, 0000-0002-4435-1844

18 Luisa Pascucci[2], 0000-0002-2562-1140

19 Cinzia Bazzucchi[2]

20 Marco Cunto[1], 0000-0002-2562-1140

21 Francesca Ricci[3]

22 Barbara Rossi[1]

23 Barbara Merlo[1], 0000-0001-7029-5404

24

25 [1]Department of Veterinary Medical Sciences, University of Bologna, Italy, via Tolara di

26 Sopra 50, 40064, Ozzano Emilia (Bologna), Italy

27 [2]Department of Veterinary Medicine, University of Perugia, via San Costanzo 4, 06126,

28 Perugia, Italy

29 [3] Immunohaematology and Transfusion Medicine, S.Orsola-Malpighi Hospital, Bologna, Italy

30

31 *Corresponding to: Prof. Eleonora Iacono: [1]Department of Veterinary Medical Sciences,

32 University of Bologna, Italy, via Tolara di Sopra 50, 40064, Ozzano Emilia (Bologna), Italy.

33 E-mail: eleonora.iacono2@unibo.it.

34 Phone number: +39-0512097567.

35

36 **Acknowledgements**

37 The Authors thank Prof. Daniele Zambelli, and Dr. Giulia Ballotta, Department of Veterinary

38 Medical Sciences, University of Bologna, for the help given in samples recovery.

Abstract

The aim of the present study was to compare canine adipose tissue mesenchymal stem cells cultured under normoxic (20% O_2) and not severe hypoxic (7% O_2) conditions in terms of marker expression, proliferation rate, differentiation potential and cell morphology. Intra-abdominal fat tissue samples were recovered from 4 dogs and cells isolated from each sample were cultured under hypoxic and normoxic conditions. Proliferation rate and adhesion ability were determined, differentiation towards chondrogenic, osteogenic and adipogenic lineages was induced; the expression of CD44, CD34, DLA-DQA1, DLA-DRA1 was determined by PCR, while flow cytometry analysis for CD90, CD105, CD45 and CD14 was carried out. The morphological study was performed by transmission electron microscopy. Canine AT-MSCs, cultured under different oxygen tensions, maintained their basic biological features. However, under hypoxia, cells were not able to form spheroid aggregates revealing a reduction of their adhesivness. In both conditions, MSCs mainly displayed the same ultrastructural morphology and retained the ability to produce membrane vesicles. Noteworthy, MSCs cultivated under hypoxya revealed a huge shedding of large complex vesicles, containing smaller round-shaped vesicles.

In our study, hypoxia partially influences the basic biological properties and the ultrastructural features of canine mesenchymal stem /stromal cells. Further studies are needed to clarify how hypoxia affects EVs production in term of amount and content in order to understand its contribution in tissue regenerative mechanisms and the possible employment in clinical applications. The findings of the present work could be noteworthy for canine as well as for other mammalian species.

Key words

canine, mesenchymal stem cells, hypoxia, electron microscopy

64 **1. Introduction**

65 Naturally occurring diseases in companion animals, such as *Canis familiaris,* can be suitable
66 models for human genetic and acquired diseases, helping to define the potential therapeutic
67 efficiency and safety of stem cells therapy (Hayes et al., 2008; Schneider et al., 2008).
68 Furthermore, the effective management of companion animals, such as dog, for their owners
69 requires sophisticated new treatments and preventive strategies. Mesenchymal stem/stromal
70 cells are the most promising candidates for tissue engineering and regenerative medicine
71 applications. To date, canine derived MSCs have been established from different tissues, such
72 as adipose tissue (Black et al., 2007), umbilical cord (Seo et al., 2009; Zucconi et al., 2010),
73 liver and bone marrow (Wenceslau et al., 2011). Adipose tissue is ubiquitously available and
74 has several advantages compared to other sources, particularly to bone marrow. In fact, it is
75 easily accessible in large quantities with minimal invasive harvesting procedures.
76 Furthermore, adipose tissue yields a high amount of MSCs (AT-MSCs) (Schäffler and
77 Büchler, 2007).
78 It is known that both local injection as well as systemic administration of MSCs result in the
79 successful engraftment of a small percentage of the injected cells in the site of the injury
80 (Chimenti et al., 2016). Consistent with these findings, some studies recently showed that the
81 regenerative ability of MSCs could be mainly attributed to the production of molecules and
82 mediators capable of activating the intrinsic regenerative process in the damaged tissues
83 inhibiting apoptosis and fibrosis, enhancing angiogenesis, stimulating mitosis and/or
84 differentiation of tissue-resident progenitor cells, and modulating the immune response
85 (Lange-Consiglio et al., 2016). These bioactive factors are freely secreted in the extracellular
86 environment or are enclosed in micrometric and nanometric vesicles (EVs) that are released
87 from MSCs (Yagi et al., 2010; Liang et al., 2014). They enclose lipids, growth factors,
88 cytokines and different kinds of RNAs that are important mediators of cell- to-cell

89 communication (Huang et al., 2013; Pascucci et al., 2014a; Pascucci et al., 2015; Crivelli et
90 al., 2017). EVs payload and their surface markers are strictly related to cell parent lineage and
91 are influenced by cell metabolic state during their biogenesis (Tetta et al., 2013). For these
92 reasons, EVs have a double role in physiological and pathological conditions, equally
93 contributing to suppress or support a pathological condition (Chaput et al., 2011), depending
94 on whether they are “good or bad” vesicles (Lo Cicero et al., 2015). Moreover, EVs exhibit
95 many of the superficial markers, cytokines, growth factors and the immune modulatory
96 properties of their origin cells (Gyorgy et al., 2015). Therefore, EVs could be used as smaller
97 cellular “alter ego”, in order to achieve innovative cell-free strategies (Gyorgy et al., 2015).
98 Furthermore, because of their capacity to encapsulate both hydrophilic and lipophilic
99 molecules and to deliver them, EVs from MSCs could be considered as drug delivery systems
100 (Bonomi et al., 2017; Pascucci et al., 2014b).
101 Several Authors reported the ultrastructural features and EVs production by adult and foetal
102 human (Budoni et al., 2013; Del Fattore et al., 2015) and equine MSCs (Pascucci et al.,
103 2014a; Pascucci et al., 2015; Lange-Consiglio et al., 2016; Iacono et al., 2017) and their
104 possible therapeutic applications (Budoni et al., 2013; Lange-Consiglio et al., 2016; Iacono et
105 al., 2017). Only one study briefly described the appearance, at transmission electron
106 microscopy, of canine bone marrow MSCs (Bonomi et al., 2017), but the EVs production by
107 these cells was no mentioned.
108 MSCs migration towards the injured tissue increases under hypoxic conditions because low
109 oxygen tension changes their surface receptors and the interaction with the damage tissue,
110 even if it is strictly related to MSCs close to the injured site (Annabi et al., 2003). Moreover,
111 AT-MSCs reside in a microenvironment with low oxygen tension (1-7%) and physiologically
112 experiences an oxygen tension lower than the atmospheric tension (20-21%) (Choi et al.,
113 2014; Choi et al., 2015). Both in humans and in dogs, MSCs are usually cultured at

114 atmospheric oxygen tension and the effects of hypoxia on proliferation, differentiation and
115 molecular profiles are contradictory (Chung et al., 2012; Lee et al., 2016). No data have been
116 reported on the effects of hypoxia on ultrastructural features and EVs production of human or
117 animal MSCs.
118 The purpose of this study was to investigate cellular proliferation, differentiation potential,
119 molecular profile, migration and adhesion ability under normoxia (21%) and hypoxia (7%).
120 Moreover, we aimed at evaluating the ultrastructural features of canine AT-MSCs and their
121 capacity to produce EVs in both culture conditions. We hypothesized that hypoxia (7%) could
122 affect cellular metabolism and consequently the release of EVs.
123

124 **2. Materials and Methods**

125 Chemicals were obtained from Sigma Aldrich (St. Louis, MO, USA) and laboratory plastic
126 ware was from Sarstedt Inc. (Newton, NC, USA) and Corning (Corning, NY, USA), unless
127 otherwise stated.
128

129 *2.1 Animals*

130 Intra-abdominal fat tissue was recovered from 7 one year old bitches referred for a routine
131 castration to the Department of Veterinary Medical Sciences, University of Bologna. The
132 written consent was given by all owners to allow the use of removed tissue for research
133 purposes and experimental procedures were approved by the Ethics Committee on animal use
134 of the Department of Veterinary Medical Sciences, University of Bologna, and by the Italian
135 Ministry of Health.
136

137 *2.2 Samples collection and cell isolation*

138 Immediately after removal, AT samples were stored in DPBS supplemented with antibiotics
139 (100 IU/ml penicillin, 100 µg/ml streptomycin) and transferred to the lab. MSCs were isolated
140 as previously described (Iacono et al., 2015). Briefly, under a laminar flow hood, tissue was
141 rinsed by repeated immersion in DPBS, weighed and minced finely (0.5 cm) by sterile
142 scissors. Minced AT was transferred into a 50ml polypropylene tube and a digestion solution,
143 containing 0.1% collagenase type I (GIBCO®, ThermoFisher Scientific, Waltham,
144 Massachusetts, USA) dissolved in DPBS, was added (1ml solution/1g tissue) mixing
145 thoroughly. This mix was kept in a 37°C water bath for 30 min and mixed every 10 min.
146 After incubation, collagenase was inactivated diluting 1:1 with DPBS supplemented with 10%
147 v/v FBS (GIBCO®, ThermoFisher Scientific, Waltham, Massachusetts, USA). The resulting
148 solution was filtered in order to discard the undigested tissue and nucleated cells were pelleted
149 at 470 *g* for 10 min. The pellet was re-suspended in culture medium [DMEM: TCM199
150 (GIBCO®, ThermoFisher Scientific, Waltham, Massachusetts, USA) = 1:1, plus 10% FBS]. It
151 was centrifuged 3 times at 470 *g* for 10 min in order to rinse cells. Cell pellet was re-
152 suspended in 1 ml of culture medium and cell concentration was evaluated by
153 haemocytometer. For plating and culturing the same cell number under hypoxic and normoxic
154 conditions, each sample was divided in 2 equal parts. The term "normoxic" indicates the
155 standard culture conditions (humidified atmosphere with 5% CO_2 and 21% O_2) while the term
156 "hypoxic" is related to a humidified atmosphere with 5% CO_2 and 7% O_2. Canine AT-MSCs
157 cultured in normoxia will be indicated as Nor-AT-MSCs whereas the ones cultured under
158 hypoxia will be indicated as Hyp-AT-MSCs.
159

160 *2.3 Cell culture and population doublings*

161 After isolation, primary cells derived from all recovered samples were plated in a 25 cm^2 flask
162 in 5 ml of culture medium at 38.5 °C under normoxic or hypoxic conditions. After 2 days of

163 in vitro culture, the medium was completely re-placed and non-adherent cells removed.
164 Hereafter the medium was changed twice a week until adherent primary MSCs reached ~80-
165 90% confluence and then they were dissociated by 0.25% trypsin, counted by a
166 haemocytometer and plated at the concentration of 5 x 10^3 cells/cm^2 as "Passage 1" (P1).
167 Cells were allowed to proliferate until 80-90% confluence before trypsinization and
168 successive passage.
169 Calculation of cell-doubling time (DT) and cell-doubling numbers (CD) was carried out
170 according to the following formulae (Rainaldi et al., 1991):
171 $CD = \ln (N_f / N_i) / \ln (2)$
172 where N_f and N_i are the final and the initial number of cells, respectively;
173 $DT = CT / CD$
174 where CT is the cell culture time.
175
176 *2.4 Adhesion and Migration Assays*
177 To define differences between Hyp-AT-MSCs and Nor-AT-MSCs, spheroid formation and
178 migration test were performed. For each group were carried out 3 replicates for each
179 experiment; all replicates were carried out at passage 3 of in vitro culture.
180 For adhesion assay, cells were cultured in 'hanging drops' (5.000 cells/drop of 25µl) for 24 h.
181 Images were acquired by a Nikon Eclipse TE 2000-U microscope. Starting from the binary
182 masks obtained by Image J software (Processing and Analysis in Java, Version 1.6,
183 imagej.nih.gov/ij/), the volume of each spheroid was computed using ReViSP
184 (sourceforge.net/projects/revisp) (Bellotti et al., 2016), a software specifically designed to
185 accurately estimate the volume of spheroids and to render an image of their 3D surface.
186 To assess cell migration potential, a scratch assay (also known as Wound-Healing assay) was
187 carried out, as previously described (Liang et al., 2007). Briefly, at 80-90 % confluence the

188 cell monolayer was scraped using a p1000 pipet tip. After washing twice with DPBS, the dish
189 was incubated for 24 h. Images were acquired both immediately after the tip-scratch (time 0;
190 T0) and after the incubation period (last time point or time 1; T1), and the distances of each
191 scratch closure were calculated by ImageJ software (Processing and Analysis in Java, Version
192 1.6, imagej.nih.gov/ij/). The migration percentages were calculated using the following
193 formula (Rossi et al., 2014):
194 [(distance at T0-distance at T1) *100]/distance at T0
195
196 *2.5 Multilineage differentiation*
197 *In vitro* differentiation potential of cells toward osteogenic, adipogenic and chondrogenic
198 lineages in different culture conditions was studied. Cells (5×10^3cells⁄cm^2) were cultured
199 under specific induction media (Table 1). As negative control, an equal number of cells was
200 cultured in expansion medium. *In vitro* differentiation potential was assessed at passage 3 of
201 culture in two replicates for three samples from each lineage. To cytologically evaluate
202 differentiation, cells were fixed with 10% formalin at room temperature (RT) and stained with
203 Oil Red O, Alcian Blue and Von Kossa for adipogenic, chondrogenic and osteogenic
204 induction, respectively. Quantitative analysis of *in vitro* differentiation was performed by
205 ImageJ (Processing and Analysis in Java, Version 1.6, imagej.nih.gov/ij/).
206
207 *2.6 Molecular Characterization*
208 Expression of specific MSCs (CD44), hematopoietic (CD34), and major histocompatibility
209 complex (DLA-DQA1, DLA-DRA1) markers was investigated by PCR analysis on
210 undifferentiated Nor-AT-MSCs and Hyp-AT-MSCs (Table 2). All tests were carried out on
211 $100x10^3$ cells, derived from three different dogs. Experiments were performed at passage 3 of
212 *in vitro* culture, except for DLA-DQA1 and DLA-DRA1: in fact, given the increasing demand
213 of MSCs for clinical use also in the canine species, the expression of DLA-DQA1 and DLA-

214 DRA1 was also studied at P0 to assess their immunologic properties. For PCR, cells were
215 snap-frozen and RNA was extracted using Nucleo Spin® RNA kit (Macherey-Nagel, Düren,
216 Germany) following the manufacturer's instructions. cDNAs were synthesized by RevertAid
217 RT Kit (ThermoFisher Scientific, Waltham, Massachusetts, USA) and used directly in PCR
218 reactions, following the instructions of Maxima Hot Start PCR Master Mix (2X)
219 (ThermoFisher Scientific, Waltham, Massachusetts, USA).
220 Canine glyceraldehyde-3-phosphate dehydrogenase (GAPDH) was employed as a reference
221 gene in each sample in order to standardize the results and to asses RNA integrity and purity.
222 Furthermore, for all primers, in order to asses sample purity, a RT- and a mix without primer
223 were analyzed.
224 PCR products were visualized with ethidium bromide on a 2% agarose gel (Bio-Rad
225 Laboratories, Inc., Hercules, California, USA.
226
227 *2.7 Flow cytometry*
228 Cytofluorimetric analysis was carried out to study the cell surface marker expression of
229 canine Nor-AT-MSCs and Hyp-AT-MSCs. At P3 cells were labeled with CD90, CD105,
230 CD14, and CD45 mouse monoclonal antibodies (all from Beckman Coulter, Milan, Italy) and
231 with isotype control mouse monoclonal antibodies. Briefly, at 80-90% of confluence, cells
232 were harvested by trypsinization after twice rinsing with DPBS and collected at a
233 concentration of 10^6 cells/ml. Fixation and permeabilization were carried out using Reagent 1
234 of Intraprep Kit (Beckman Coulter, Milan, Italy). Flow cytometry was performed using
235 FC500 two-laser equipped cytometer (Beckman Coulter, Milan, Italy). Coniugated-specific
236 antibodies or isotype-matched control mouse immunoglobulin G are listed in Table 3. Cross-
237 reactivity of the antibodies used was screened using cultured human and canine MSCs.
238 Incubated cells with isotype-specific IgGs were used as control cells in order to establish the

239 background signal. Furthermore, to verify cross-reactivity, control on circulating canine
240 lymphocytes was carried out. The similarity of CD markers was also identified by comparing
241 the amino acid sequences using Basic Local Alignment Search Tool (BLAST). Results were
242 further analyzed with the CXP dedicated program.
243
244 *2.8 Transmission Electron Microscopy (TEM)*
245 Ultrastructural investigation was carried out on canine Nor-AT-MSCs (n=3) and Hyp-AT-
246 MSCs (n=3) at P3 of culture. At this time, the cells were detached from the flask by trypsin-
247 EDTA, centrifuged at 600 *g* for 10 minutes to remove the medium and fixed with 2.5%
248 glutaraldehyde in 0.1 M phosphate buffer (PB), pH 7.3, for 1 h at room temperature. They
249 were subsequently washed twice in PB and post-fixed with 2% osmium tetroxide dissolved in
250 0.1 M PB, pH 7.3, for 1 h at room temperature. Cells were finally dehydrated in a graded
251 series of ethanol up to absolute, pre-infiltrated and embedded in Epon 812 (Electron
252 Microscopy Sciences, Hatfield, Pa, USA). Ultrathin sections (90 nm) were mounted on 200-
253 mesh copper grids, stained with uranyl acetate and lead citrate, and examined by means of a
254 Philips EM 208, equipped with a digital camera.
255
256 *2.9 Statistical analysis*
257 CDs, DTs and percentages of migration are expressed as mean ± standard deviation.
258 Statistical analyses were performed using IBM SPSS Statistics 23 (IBM Corporation,
259 Armonk, New York, USA). Data were analysed, for normal distribution, using a Shapiro-
260 Wilk test. For growth curve, DTs and CDs were analysed using Student's T Test for paired
261 variables. To compare single culture passage DTs one-way ANOVA and post hoc Tuckey test
262 were applied. Data recorded from scratch test were analysed by Student's T test for paired

263 variables, while the 3D spheroid volumes were compared using Wilcoxon test, due to their
264 non-normal distribution. Significance was assessed for $P<0.05$.
265
266 ## 3. Results
267
268 *3.1 Cell culture, in vitro differentiation and phenotype characterization*
269 Adherent cells with the characteristic spindle-shaped morphology were isolated from all
270 samples and cultivated both under normoxia and hypoxia condition. For all samples, in both
271 culture conditions, undifferentiated cells were cultured until P5. At P5, total CDs registered
272 for Nor-AT-MSCs and Hyp-AT-MSCs were not statistically different (12.9±3.4 vs 12.7±3.2;
273 $P>0.05$; Fig.1A) ($P>0.05$). No statistically significant differences ($P>0.05$) were found
274 between total DTs in Nor-AT-MSCs and Hyp-AT-MSCs (3.58±2.14 vs 3.53±2.13 days
275 respectively; $P>0.05$; Fig.1B); the only difference observed was at the second passage of *in*
276 *vitro* culture, when Nor-AT-MSCs DT (3.6 ± 1.4 days) was higher than Hyp-AT-MSCs DT
277 (2.9 ± 0.9 days) (Fig.1B; $P<0.05$). Analysing DTs at different passage in the same culture
278 group, both in Nor-AT-MSCs and Hyp-AT-MSCS a statistically significant increase was
279 observed starting from P3 (Fig.1B; $P<0.05$).
280 As showed in Fig. 2A, no significant differences ($P>0.05$) in the migration abilities were
281 observed between Nor-AT-MSCs (68.5 ± 10.8 %) and Hyp-AT-MSCs (76.9 ± 10.0%); on the
282 contrary, while Nor-AT-MSCs cultured in 'hanging drops' were able to form spheroids, Hyp-
283 AT-MSCs did not form a compact spheroid (Fig.2B). For these reasons a statistically
284 significant difference was found between spheroid volumes: the spheroid formed by Hyp-AT-
285 MSCs was twice in volume compared to that formed by Nor-AT-MSCs ($P<0.05$).
286 In order to characterize canine Nor-AT-MSCs and Hyp-AT-MSCs, PCRs were performed for
287 CD34 as hematopoietic marker, for CD44 as MSC marker, for dog leukocytes antigens DLA-
288 DQA1 and DLA-DRA1. CD44 expression was detected in cells cultured under both

289 conditions, while no samples expressed CD34 (Fig.3A). DLA-DQA1 was weakly expressed
290 only at P0, while DLA-DRA1 was not expressed by any sample, at each culture passage
291 examined (Fig.3A).
292 Cells cultured under both atmosphere conditions resulted positive for mesenchymal markers
293 CD90, and CD105. The haematopoietic markers CD14 and CD45 were expressed in low
294 percentages (<20%) in all samples, with a significant difference (P<0.05) in the expression of
295 CD45 between Nor-AT-MSCs and Hyp-AT-MSCs (8.4 ± 1.2 vs 13.0 ± 0.5) (Fig.3B).
296 As well as the molecular characterization seems not to be affected by *in vitro* culture
297 conditions, also the ability of cell to differentiate *in vitro* is similar. In fact, both Nor-AT-
298 MSCs and Hyp-AT-MSCs, cultured in induction media were able to differentiate toward
299 osteogenic, chondrogenic and adipogenic direction (Fig.4).
300
301 *3.2 Transmission Electron Microscopy (TEM)*
302 When analyzed by TEM, cells cultivated in both experimental conditions were characterized
303 by a unique euchromatic nucleus with irregular profile and one or more prominent nucleoli
304 (Figg. 5A, 6A). Cytoplasm was populated by abundant free ribosomes. Apart from some flat
305 profiles of RER, in both cell samples the cisternal space of the RER was often greatly
306 distended (Figg. 5C, 6B). A consistent number of mitochondria was observed in both
307 samples. They mostly appeared elongated and were characterized by normal cristae.
308 Membrane integrity was maintained (Figg. 5B, 6B). Golgi apparatus was well developed and
309 typically included flattened cisternae, transport vesicles, and heterogeneous sized vacuoles,
310 some of which were very large and filled with either electron-lucent or fine granular material
311 (Figg. 5B, 6C). The endo-lysosomal apparatus showed a variety of appearances;
312 multivesicular bodies (MVBs) and endo-lysosomes were quite abundant. MVBs appeared as
313 large vacuoles more than 500 nm in diameter containing 30 to 100 nm wide intraluminal

314 small vesicles. Maturation of endosomes was reflected by the progressive increasing number
315 of intraluminal vesicles. Endo-lysosomes, on the other hand, appeared as vacuolar structures
316 characterized by nano-vesicles, typical of late endosomes, mixed with aggregates of electron-
317 dense material and occasional para-crystalline formations. Endo-lysosomes were present in
318 both cell types, but they were more abundant in cells cultured under hypoxia (Figg. 5C, 5D,
319 6B). Autophagic vacuoles were occasionally seen in Hyp-AT-MSCs. Cellular membrane
320 showed an irregular profile due to the presence of cytoplasmic pseudopodial evaginations and
321 to the occurrence of large complex vesicles shedding from the cell surface. This latter
322 phenomenon appeared more evident in Hyp-AT-MSCs where large electron-lucent vesicles
323 frequently budded from the cell surface. These vesicles were 2000 nm or even larger in
324 diameter and contained round-shaped 300 to 500 nm wide vesicles inside their lumen (Figg.
325 5F, 6E, 6F). Under both atmospheric conditions the extracellular space was populated by
326 numerous vesicles of heterogeneous size (Figg. 5E, 6D).
327

328 ## 4. Discussion

329 The use of MSCs for regenerative medicine has been proposed in human and veterinary
330 species (Fortier and Travis, 2011). The most studied source of MSCs is bone marrow; in
331 particular, some Authors suggested that it may be a superior source of MSCs for osteogenesis
332 since, in this microenvironment, cells are pre-committed towards the osteogenic lineage (Noël
333 et al., 2008). Adipose tissue is another ideal source of MSCs: it is abundant and can be easily
334 obtained from several body's regions with minimal side effects for donor (Tapp et al., 2009).
335 Initially, the beneficial effect of MSCs was thought to derive from their proliferation and
336 differentiation (Kopen et al., 1999). However, the observation that only a small number of
337 transplanted cells survive and integrate into host damaged tissue has highlighted the
338 possibility that an alternative mechanism exists. Today, it is widespread opinion that MSCs

339 create optimal environmental conditions for tissue regeneration via a paracrine mechanism
340 (Pascucci et al., 2014a; Crivelli et al., 2017). In particular, MSCs produce trophic factors,
341 cytokines and signaling molecules, able to influence angiogenesis, cell proliferation,
342 apoptosis and even recruitment of resident stem cells (Pascucci et al., 2014a). The complex
343 interaction between MSCs and tissue microenvironment might involve both soluble factors
344 and production of extracellular vesicles containing various molecules (György et al., 2011).
345 The importance of tissue environmental factors, like oxygen tension, has been previously
346 studied in human MSCs in relation to differentiation capability (Cicione et al., 2013) and cell
347 growth (Hung et al., 2012). *In vitro,* cell cultures are generally carried out under 20-21% O_2,
348 known as normoxia, but it does not replicate the physiological or pathological hypoxia
349 corporeal conditions (He et al., 2007). For this reason, recently many research groups have
350 been started to compare culture and differentiation of MSCs in normoxia and hypoxia (5%
351 O_2) or severe hypoxia (1-3% O_2) (Buravkova et al., 2014). Results obtained in the present
352 study are similar to those reported previously by Chung et al. (2012) about canine AT-MSCs
353 growth rate in normoxia (21%) and in hypoxia (7%), but different from those reported by
354 other Authors (Lee et al., 2016). This confirms, as already reported in humans, the disparity in
355 results obtained culturing cells under hypoxic conditions (Choi et al., 2017). Because the
356 effects of hypoxia on proliferation rate of AT-MSCs could be influenced not only by oxygen
357 rate but also by other different factors, such as area of body from which it was removed,
358 different sexes and age of donor, further studies are needed to verify if this could be true also
359 in canine species.
360 Beyond the growth curve, migration ability is an important feature of MSCs because of its
361 fundamental significance for systemic application (Li et al., 2009; Burk et al., 2013). No
362 differences were found between Nor-AT-MSCs and Hyp-AT-MSCs in migration ability.
363 Since the adhesion capability is related and enhanced to differentiation potential (Pasquinelli

364 et al., 2007; Wang et al., 2009), in the present study, for the first time in canine species,
365 spheroid formation *in vitro* was assessed using the hanging drop method. Cells cultured under
366 normoxia showed a higher adhesion ability, forming smaller spheroids However, no
367 difference were observed in differentiation ability of cells cultured in induction medium in
368 21% and 7% O_2. This could be related to the further reduction of oxygen within the
369 micromasses which therefore requires a further adaptation of the cells to the new condition.
370 As previously reported (Chung et al., 2012; Lee et al., 2016), also under our culture
371 conditions canine AT-MSCs maintain their stemness and the characteristic molecular profile.
372 In fact, both Nor and Hyp-AT-MSCs expressed CD44 and did not express CD34, a
373 hematopoietic marker. Furthermore, by RT-PCR, we demonstrated that, at P3 of *in vitro*
374 culture in normoxia and hypoxia, canine AT-MSCs did not express DLA-DRA1 and DLA-
375 DQA1. Furthermore, as previously reported in canine MSCs (Seo et al., 2009; Filioli Uranio
376 et al., 2014), we found a very weak expression of DLA-DRA1 at P0. We could postulate that
377 the expression of these markers has been lost during the first passages in canine AT-MSCs,
378 confirming the low immunogenicity of these populations of cells and supporting their possible
379 use for allo- and xenotransplantation.
380 With the exception of a few reports, MSCs morphology has been widely disregarded in the
381 past years (Budoni et al., 2013; Pascucci et al., 2014a; Del Fattore et al., 2015; Pascucci et al.,
382 2015; Lange-Consiglio et al., 2016; Iacono et al., 2017). In this manuscript, we discussed the
383 establishment of MSCs cultures from canine adipose tissue and described, for the first time,
384 their fine structure by transmission electron microscopy. Furthermore, since also in canine
385 species it was demonstrated that oxygen concentration is an important component of stem cell
386 niche (Chung et al., 2012; Lee et al., 2016) but no data are present on the effects of oxygen
387 tension on cellular components and their ability to produce EVs, we ascertained, by means of
388 electron microscopy, that canine AT-MSCs constitutively produce EVs under different

389 oxygen tensions and we compared the effect of normoxia (21%) and hypoxia (7%) on canine
390 AT-MSCs fine structure. The ultrastructural morphology was mainly maintained in Hyp-AT-
391 MSCs when compared with Nor-AT-MSCs. Canine AT-MSCs were homogeneous in shape
392 and dimensions and presented a large, irregular nucleus with multiple nucleoli, as a sign of
393 intense metabolic activity. This was confirmed by a consistent number of mitochondria. The
394 main differences between Hyp-AT-MSCs and Nor-AT-MSCs attained the presence of
395 occasional autophagosomes, the increased number of endolysosomes and the abundance of
396 large complex vesicles budding from the cell surface and containing smaller vesicles in cells
397 cultured in 7% O_2. This particular kind of EVs has never been described before in the
398 literature in dogs, but it was frequently observed by the authors in MSCs of different species
399 and tissue sources (Pascucci et al., 2014a; Pascucci et al., 2015). Concerning endolysosomes
400 and autophagosomes, it could be hypothesized that the hypoxic environment could induce a
401 mild injury because of the reduced oxygen availability, followed by the digestion of damaged
402 cell components. Therefore, autophagy may be interpreted as a reactive behavior of the cell to
403 the adverse environmental conditions. The increased number of large complex vesicles
404 budding from the cell surface and containing smaller vesicles, and the great quantity of MVBs
405 and extracellular vesicles led to hypothesize that the high metabolic and synthetic activity
406 typical of MSCs is enhanced in Hyp-AT-MSCs respect to cells cultured in normoxia. This is
407 supported by the presence of an unchanged synthetic apparatus formed by the euchromatic
408 nucleus, by a great number of free ribosomes, by a well developed RER and Golgi apparatus.
409 This last one, additionally, produce large vacuoles containing a fine granular material that
410 could be addressed to secretion. Examination of cell monolayers by TEM, allowed to
411 hypothesize that EVs production could be influenced by the *in vitro* culture oxygen tension.
412 Particularly, we observed that in cells cultured under low oxygen tension, large complex EVs
413 seems to be more numerous. As previously speculated (Pascucci et al., 2015), it is possible

414 that this kind of vesicles encloses smaller vesicles that, in a first phase, are grouped in specific
415 areas, underneath the plasma membrane and are then exocytosed through an apocrine-like
416 secretion. In this way, cells are able to package a large amount of cargo enclosed inside large
417 complex vesicles. Even if their content needs still to be characterized, it could be speculated
418 that it may be able to modulate, at the same time, different biological pathways so inducing a
419 strong and polymorfous environmental response.
420 In equine species, it was recently demonstrated that AT-MSCs EVs are involved in
421 modulation of different stages of angiogenesis (Pascucci et al., 2014a). Different Authors
422 stated that hypoxia increases the secretion of angiogenic factors and that the medium
423 conditioned by hypoxic-treated cells may enhance angiogenesis and perfusion in nude mice
424 with ischemic hindlimbs (Rehman et al., 2004; Stubbs et al., 2012). Furthermore, hypoxic-
425 treated cells were found to increase secretion of antitapoptotic factors, such as IL-6: this factor
426 has been demonstrated to inhibit cardiomyocyte apoptosis and reduce infarct size (Matsushita
427 et al., 2005; Jung et al., 2009; Przybyt et al., 2013). Recently, it was demonstrated that canine
428 bone marrow MSCs loaded with paclitaxel (PTX) are able to release it affecting in vitro
429 cancer cells proliferation (Bonomi et al., 2017). PTX release could be partly mediated by
430 EVs, as previously demonstrated in an in vitro murine model. Considering that tumor
431 environment is often characteristically hypoxic, the possible therapeutic use of MSC
432 cultivated under hypoxia to produce EVs to be used as drug delivery system deserves a
433 careful further study also in canine species.
434 The results of the present study indicate that MSCs from canine adipose tissue constitutively
435 produce EVs that may be responsible of their paracrine activity. Furthermore, the EVs
436 production seems to be influenced by *in vitro* culture oxygen tension. There is need for further
437 mechanistic studies of hypoxia to elucidate its influence not only on EVs production but also
438 in their composition in view of clinical and pharmaceutical applications.

439

440 **5. Author's declaration of interest:** No competing interests have been declared.

441

442

443

444 **6. References**

445 Annabi B, Lee YT, Turcotte S, Naud E, Desrosiers RR, Champagne M, Eliopoulos N,
446 Galipeau J, Béliveau R (2003) Hypoxia promotes murine bone-marrow-derived stromal cell
447 migration and tube formation. Stem Cells 21:337-347. https://doi.org/10.1634/stemcells.21-3-
448 337.
449 Bellotti C, Duchi S, Bevilacqua A, Lucarelli E, Piccinini F (2016) Long term morphological
450 characterization of mesenchymal stromal cells 3D spheroids built with a rapid method based
451 on entry-level equipment. Cytotechnology 68:2479-2490. https://doi.org/ 10.1007/s10616-
452 016-9969-y.
453 Black LL, Gaynor J, Gahring D, Adams C, Aron D, Harman S, Gungerich DA, Harman R
454 (2007) Effect of adipose-derived mesenchymal stem and regenerative cells on lameness in
455 dogs with chronic osteoarthritis of the coxofemoral joints: a randomized, double-blinded,
456 multi- center, controlled trial. Vet Ther 8:272-284.
457 Bonomi A, Ghezzi E, Pascucci L, Aralla M, Ceserani V, Pettinari L, Coccè V, Guercio A,
458 Alessandri G, Parati E, Brini AT, Zeira O, Pessina A (2017) Effect of canine mesenchymal
459 stromal cells loaded with paclitaxel on growth of canine glioma and human glioblastoma cell
460 lines. Vet J 223:41-47. https://doi.org/10.1016/j.tvjl.2017.05.005.
461 Budoni M, Fierabracci A, Luciano R, Petrini S, Di Ciommo V, Muraca M (2013) The
462 immunosuppressive effect of mesenchymal stromal cells on B lymphocytes is mediated by
463 membrane vesicles. Cell Transplant 22:369-379. https://doi.org/10.3727/096368911X582769.
464 Buravkova LB, Andreeva ER, Gogvadze V, Zhivotovsky B (2014) Mesenchymal stem cells
465 and hypoxia: Where are we? Mitochondrion 19PtA:105-112.
466 https://doi.org/10.1016/j.mito.2014.07.005.

467 Burk J, Ribitsch I, Gittel C, Juelke H, Kasper C, Staszyk C, Brehm W (2013) Growth and
468 differentiation characteristics of equine mesenchymal stromal cells derived from different
469 sources. Vet J 195:98-106. https://doi.org/10.1016/j.tvjl.2012.06.004.
470 Chaput N, Thery C (2011) Exosomes: immune properties and potential clinical
471 implementations. Semin Immunopathol 33:419-440. https://doi.org/10.1007/s00281-010-
472 0233-9.
473 Chimenti I, Smith RR, Li TS, Gerstenblith G, Messina E, Giacomello A, Marbán E (2016)
474 Relative roles of direct regeneration versus paracrine effects of human cardiosphere-derived
475 cells transplanted into infarcted mice. Circ Res 106:971-980.
476 https://doi.org/10.1161/CIRCRESAHA.109.210682.
477 Choi JR, Pingguan-Murphy B, Wan Abas WA, Yong KW, Poon CT, Noor Azmi MA, Omar
478 SZ, Chua KH, Wan Safwani WK (2014) Impact of low oxygen tension on stemness,
479 proliferation and differentiation potential of human adipose-derived stem cells., Biochem
480 Biophys Res Commun 448:218-224. https://doi.org/10.1016/j.bbrc.2014.04.096.
481 Choi JR, Pingguan-Murphy B, Wan Abas WA, Yong KW, Poon CT, Noor Azmi MA, Omar
482 SZ, Chua KH, Xu F, Wan Safwani WK (2015) In situ normoxia enhances survival and
483 proliferation rate of human adipose tissue-derived stromal cells without increasing the risk of
484 tumour genesis. POne 10:e0115034. https://doi.or/10.1371/journal.pone.0115034
485 Choi JR, Yong KW, Wan Safwani WKZ (2017) Effect of hypoxia on human adipose-
486 derived mesenchymal stem cells and its potential clinical applications. Cell Mol Life Sci
487 74:2587-2600. https://doi.org/10.1007/s00018-017-2484-2
488 Chung DA, Hayashi K, Chrisoula A, Toupadakis CA, Wong A, Yellowley CE (2012)
489 Osteogenic proliferation and differentiation of canine bone marrow and adipose tissue derived
490 mesenchymal stromal cells and the influence of hypoxia. Res Vet Sci 92:66-75.
491 https://doi.org/10.1016/j.rvsc.2010.10.012.

492 Cicione C, Muiños-López E, Hermida-Gómez T, Fuentes-Boquete I, Díaz-Prado S, Blanco FJ
493 (2013) Effects of severe hypoxia on bone marrow mesenchymal stem cells differentiation
494 potential. Stem Cells Int:232896. http://dx.doi.org/10.1155/2013/232896.
495 Crivelli B, Chlapanidas T, Perteghella S, Lucarelli E, Pascucci L, Brini AT, Ferrero I,
496 Marazzi M, Pessina A, Torre ML (2017) Mesenchymal stem/stromal cell extracellular
497 vesicles: From active principle to next generation drug delivery system. J Control Release
498 262:104-117. https://doi.org/10.1016/j.jconrel.2017.07.023.
499 Del Fattore A, Luciano R, Pascucci L, Goffredo BM, Giorda E, Scapaticci M, Fierabracci A,
500 Muraca M (2015) Immunoregulatory effects of mesenchymal stem cell-derived extracellular
501 vesicles on T lymphocytes. Cell Transplant 24:2615-2627.
502 https://doi.org/10.3727/096368915X687543.
503 Filioli Uranio M, Dell'Aquila ME, Caira M, Guaricci AC, Ventura M, Catacchio CR, Ventura
504 M, Cremonesi F (2014) Characterization and in vitro differentiation potency of early-passage
505 canine amnion- and umbilical cord-derived mesenchymal stem cells as related to gestational
506 age. Mol Reprod Dev 81:539-551. https://doi.org/10.1002/mrd.21311.
507 Fortier LA, Travis AJ (2011) Stem cells in veterinary medicine. Stem Cell Res Ther 2:9.
508 https://doi.org/10.1186/scrt50
509 Gyorgy B, Hung ME, Breakefield XO (2015) Therapeutic applications of extracellular
510 vesicles: clinical promise and open questions. Ann Rev Pharmacol Toxicol 55:439-464.
511 Hayes B, Fagerlie SR, Ramakrishnan A, Baran S, Harkey M, Graf L, Bar M, Bendoraite A,
512 Tewari M, Torok-Storb B (2008) Derivation, characterization, and in vitro differentiation of
513 canine embryonic stem cells. Stem Cells 26:465-473. https://doi.org/10.1634/stemcells.2007-
514 0640.
515 He MC, Li J, Zhao CH (2007) Effect of hypoxia on mesenchymal stem cells - review. J Exp
516 Hematol Chinese Ass Pathophys 15:433-436.

517 Huang YC, Parolini O, Deng L (2013) The potential role of microvesicles in mesenchymal
518 stem cell-based therapy. Stem Cells Dev 15:841-844. https://doi.org/10.1089/scd.2012.0631.
519 Hung SP, Ho JH, Shih YR, Lo T, Lee OK (2012) Hypoxia promotes proliferation and
520 osteogenic differentiation potentials of human mesenchymal stem cells. J Orthop Res 30:260-
521 266. https://doi.org/10.1002/jor.21517.
522 Iacono E, Merlo B, Romagnoli N, Rossi B, Ricci F, Spadari A (2015) Equine Bone Marrow
523 and Adipose Tissue Mesenchymal Stem Cells: Cytofluorimetric Characterization, In Vitro
524 Differentiation, and Clinical Application. J Eq Vet Sci 35:130-140.
525 https://doi.org/10.1016/j.jevs.2014.12.010.
526 Iacono E, Pascucci L, Rossi B, Bazzucchi C, Lanci A, Ceccoli M, Merlo B (2017)
527 Ultrastructural characteristics and immune profile of equine MSCs from fetal adnexa.
528 Reproduction 154:509-519. https://doi.org/10.1530/REP-17-0032.
529 Jung DI, Ha J, Kang BT, Kim JW, Quan FS, Lee JH, Woo EJ, Park HM (2009) A comparison
530 of autologous and allogenic bone marrow-derived mesenchymal stem cell transplantation in
531 canine spinal cord injury. J Neurol Sci 285:67-77. https://doi.org/10.1016/j.jns.2009.05.027.
532 Kopen GC, Prockop DJ, Phinney DG (1999) Marrow stromal cells migrate throughout
533 forebrain and cerebellum, and they differentiate into astrocytes after injection into neonatal
534 mouse brains. Proc Nat Acad Sci U S A 96:10711-10716.
535 https://doi.org/10.1073/pnas.96.19.10711.
536 Lange-Consiglio A, Perrini C, Tasquier R, Deregibus MC, Camussi G, Pascucci L, Marini
537 MG, Corradetti B, Bizzaro D, De Vita B, Romele P, Parolini O, Cremonesi F (2016) Equine
538 Amniotic Microvesicles and Their Anti-Inflammatory Potential in a Tenocyte Model In Vitro.
539 Stem Cells Dev 25:610-621. https://doi.org/10.1089/scd.2015.0348.

540 Lee J, Byeon JS, Lee KS, Gu NY, Lee GB, Kim HR, Cho IS, Cha SH (2016) Chondrogenic
541 potential and anti-senescence effect of hypoxia on canine adipose mesenchymal stem cells.
542 Vet Res Commun 40:1-10. https://doi.org/10.1007/s11259-015-9647-0.
543 Li G, Zhang X, Wang H, Wang X, Meng CL, Chan CY, Yew DT, Tsang KS, Li K, Tsai SN,
544 Ngai SM, Han ZC, Lin MC, He ML, Kung HF (2009) Comparative proteomic analysis of
545 mesenchymal stem cells derived from human bone marrow, umbilical cord and placenta:
546 implication in the migration. Proteomics 9:20-30. https://doi.org/10.1002/pmic.200701195.
547 Liang CC, Park AY, Guan JL (2007) In vitro scratch assay: a convenient and inexpensive
548 method for analysis of cell migration in vitro. Nat Protoc 2:329-333.
549 https://doi.org/10.1038/nprot.2007.30.
550 Liang X, Ding Y, Zhang Y, Tse FT, Lian Q (2014) Paracrine mechanisms of mesenchymal
551 stem cell-based therapy: current status and perspectives. Cell Transplant 23:1045-1059.
552 https://doi.org/10.3727/096368913X667709.
553 Lo Cicero A, Stahl PD, Raposo G (2015) Extracellular vesicles shuffling intercellular
554 messages: for good or for bad. Curr Opin Cell Biol 35:69-77.
555 https://doi.org/10.1016/j.ceb.2015.04.013.
556 Matsushita K, Iwanaga S, Oda T, Kimura K, Shimada M, Sano M, Umezawa A, Hata J,
557 Ogawa S (2005) Interleukin-6/soluble interleukin-6 receptor complex reduces infarct size via
558 inhibiting myocardial apoptosis. Lab Invest 85:1210-1223.
559 https://doi.org/10.1038/labinvest.3700322.
560 Noël D, Caton D, Roche S, Bony C, Lehmann S, Casteilla L, Jorgensen C, Cousin B (2008)
561 Cell specific differences between human adipose-derived and mesenchymal-stromal cells
562 despite similar differentiation potentials. Exp Cell Res 314:1575-1584.
563 https://doi.org/10.1016/j.yexcr.2007.12.022.

564 Pascucci L, Alessandri G, Dall'Aglio C, Mercati F, Coliolo P, Bazzucchi C, Dante S, Petrini
565 S, Curina G, Ceccarelli P (2014a) Membrane vesicles mediate pro-angiogenic activity of
566 equine adipose-derived mesenchymal stromal cells. Vet J 202:361-366.
567 https://doi.org/10.1016/j.tvjl.2014.08.021.

568 Pascucci L, Coccè V, Bonomi A, Ami D, Ceccarelli P, Ciusani E, Viganò L, Locatelli A,
569 Sisto F, Doglia SM, Parati E, Bernardo ME, Muraca M, Alessandri G, Bondiolotti G,Pessina
570 A (2014b) Paclitaxel is incorporated by mesenchymal stromal cells and released in exosomes
571 that inhibit in vitro tumor growth: a new approach for drug delivery. J Control Release
572 192:262-270. https://doi.org/10.1016/j.jconrel.2014.07.042.

573 Pascucci L, Dall'Aglio C, Bazzucchi C, Mercati F, Mancini MG, Pessina A, Alessandri G,
574 Giammarioli M, Dante S, Brunati G, Ceccarelli P (2015) Horse adipose-derived mesenchymal
575 stromal cells constitutively produce membrane vesicles: a morphological study. Histol
576 Histopathol 30:549-557. https://doi.org/10.14670/HH-30.549.

577 Pasquinelli G, Tazzari PL, Ricci F, Vaselli C, Buzzi M, Conte R, Orrico C, Foroni L, Stella
578 A, Alviano F, Bagnara GP, Lucarelli (2007) Ultrastructural characteristics of human
579 mesenchymal stromal (stem) cells derived from bone marrow and term placenta. Ultrastr
580 Pathol 31:23-31. https://doi.org/10.1080/01913120601169477.

581 Przybyt E, Krenning G, Brinker MG, Harmsen MC (2013) Adipose stromal cells primed with
582 hypoxia and inflammation enhance cardiomyocyte proliferation rate in vitro through STAT3
583 and Erk1/2. J Transl Med 11:39. https://doi.org/10.1186/1479-5876-11-39.

584 Rainaldi G, Pinto B, Piras A, Vatteroni L, Simi S, Citti L (1991) Reduction of proliferative
585 heterogeneity of CHEF18 Chinese hamster cell line during the progression toward
586 tumorigenicity. In Vitro Cell Dev Biol 27:949-952.

587 Rehman J, Traktuev D, Li J, Temm-Grove CJ, Bovenkerk JE, Pell CL, Johnstone BH,
588 Considine RV, March KL (2004) Secretion of angiogenic and antiapoptotic factors by human

589 adipose stromal cells. Circulation 109:1292-1298.
590 https://doi.org/10.1161/01.CIR.0000121425.42966.F1.
591 Rossi B, Merlo B, Colleoni S, Iacono E, Tazzari PL, Ricci F, Lazzari G, Galli C (2014).
592 Isolation and in vitro characterization of bovine amniotic fluid derived stem cells at different
593 trimesters of pregnancy. Stem Cell Rev 10:712-724. https://doi.org/10.1007/s12015-014-
594 9525-0.
595 Schäffler A, Büchler C (2007) Concise review: adipose tissue-derived stromal cells - basic
596 and clinical implications for novel cell-based therapies. Stem Cells 25:818-827.
597 https://doi.org/10.1634/stemcells.2006-0589.
598 Schneider MR, Wolf E, Braun J, Kolb HJ, Adler H (2008) Canine embryo-derived stem cells
599 and models for human diseases. Hum Mol Genet 17: R42-47.
600 https://doi.org/10.1093/hmg/ddn078.
601 Seo MS, Jeong YH, Park JR, Park SB, Rho KH, Kim HS, Yu KR, Lee SH, Jung JW, Lee YS,
602 Kang KS (2009) Isolation and characterization of canine umbilical cord blood-derived
603 mesenchymal stem cells. J Vet Sci 10:181-187. https://doi.org/10.4142/jvs.2009.10.3.181.
604 Stubbs SL, Hsiao ST, Peshavariya HM, Lim SY, Dusting GJ, Dilley RJ (2012) Hypoxic
605 preconditioning enhances survival of human adipose-derived stem cells and conditions
606 endothelial cells in vitro. Stem Cells Dev 21:1887-1896.
607 https://doi.org/10.1089/scd.2011.0289.
608 Tapp H, Hanley EN Jr, Patt JC, Gruber HE (2009) Adipose-derived stem cells:
609 characterization and current application in orthopaedic tissue repair. Exp Biol Med 234:1-9.
610 https://doi.org/10.3181/0805/MR-170.
611 Tetta C, Ghigo E, Silengo L, Deregibus MC, Camussi G (2013) Extracellular vesicles as an
612 emerging mechanism of cell-to-cell communication. Endocrine 44:11-19.
613 https://doi.org/10.1007/s12020-012-9839-0.

614 Wang W, Itaka K, Ohba S, Nishiyama N, Chung UI, Yamasaki Y, Kataoka K (2009) 3D
615 spheroid culture system on micropatterned substrates for improved differentiation efficiency
616 of multipotent mesenchymal stem cells. Biomaterials 30:2705-2715.
617 https://doi.org/10.1016/j.biomaterials.2009.01.030
618 Wenceslau CV, Miglino MA, Martins DS, Ambrosio CE, Lizier NF, Pignatari GC, Kerkis I
619 (2011) Mesenchymal progenitor cells from canine fetal tissues: yolk sac, liver, and bone
620 marrow. Tissue Eng Part A 17:2165-2176. https://doi.org/10.1089/ten.tea.2010.0678.
621 Yagi H, Soto-Gutierrez A, Parekkadan B, Kitagawa Y, Tompkins RG, Kobayashi N,
622 Yarmush ML (2010) Mesenchymal stem cells: mechanisms of immunomodulation and
623 homing. Cell Transplant 19:667-679. https://doi.org/10.3727/096368910X508762.
624 Zucconi E, Vieira NM, Bueno DF, Secco M, Jazedje T, Ambrosio CE, Passos-Bueno MR,
625 Miglino MA, Zatz M (2010) Mesenchymal stem cells derived from canine umbilical cord
626 vein-A novel source for cell therapy studies. Stem Cells Dev 19:395-402.
627 https://doi.org/10.1089/scd.2008.0314.
628

629 **Figure legends:**

630 **Fig. 1.** Total Cell Doublings (A) and Doubling times (B) of Nor-AT-MSCs and Hyp-AT-

631 MSCs over five passages of culture. A vs b, and * vs **: $P<0.05$.

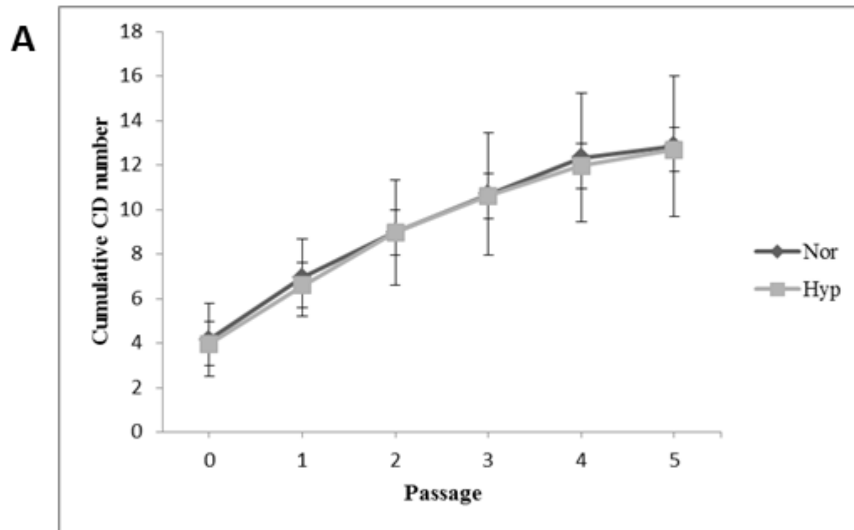
A
Cumulative CD number
18
16
14
12
10
8
6
4
2
0
0
1
2
3
4
5
Passage
Nor
Hyp

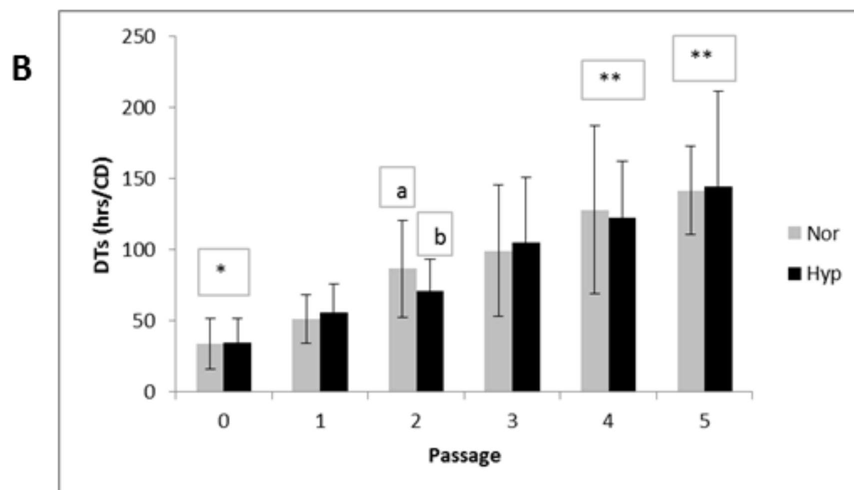
B
DTs (hrs/CD)
250
200
150
100
50
0
*
a
b
**
**
0
1
2
3
4
5
Passage
Nor
Hyp

633 **Fig. 2.** A: Scratch assay on Nor-AT-MSCs and Hyp-AT-MSCs at T0 and after 24 h (T1) of
634 cell growth (Magnification 4X, scale bar 100 μm). B: Adhesion assay: Volume reconstruction
635 and visualization of a Nor- and Hyp-AT-MSC spheroid, obtained after 48 h of hanging drop
636 culture (Magnification 10x, scale bar 10μm).

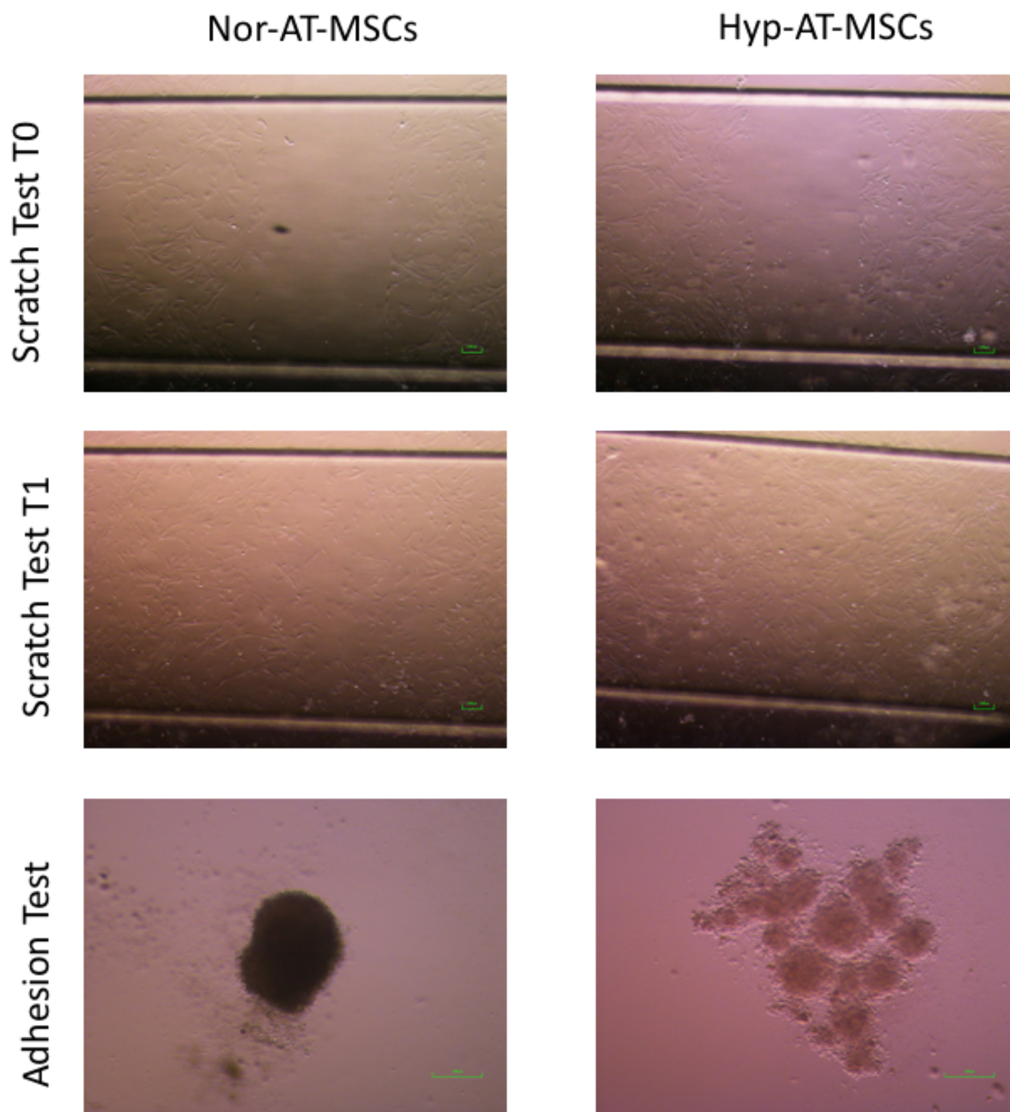

637

638 **Fig. 3**. A: Representative RT-PCR analysis of gene expression in canine AT-MSCs cultured
639 in different oxygen atmospheres. CD44, CD34 expression was evaluated on samples at P3
640 whereas dog leukocytes antigens expression was studied both at P0 and at P3. B: Flow
641 cytometric analysis. Nor-AT-MSCs and Hyp-AT-MSCs samples analyzed for different
642 antigens expression (CD90, CD105, CD14, CD45) by FACS analysis.

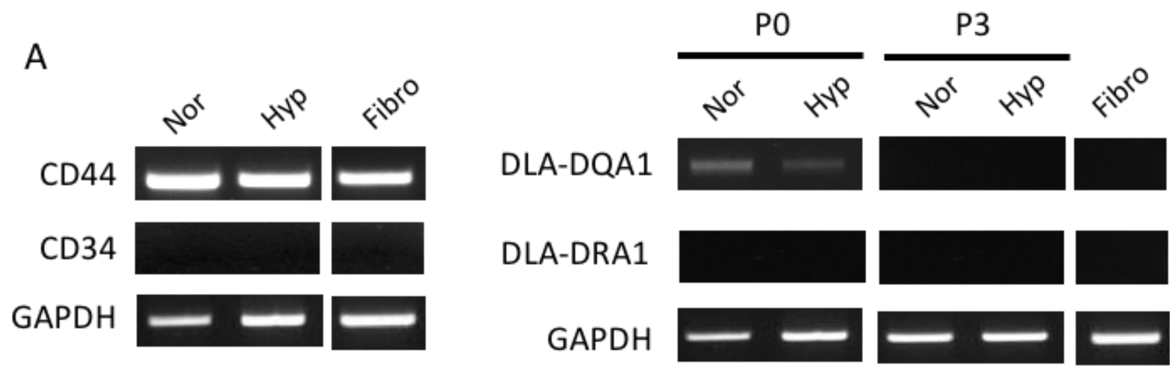

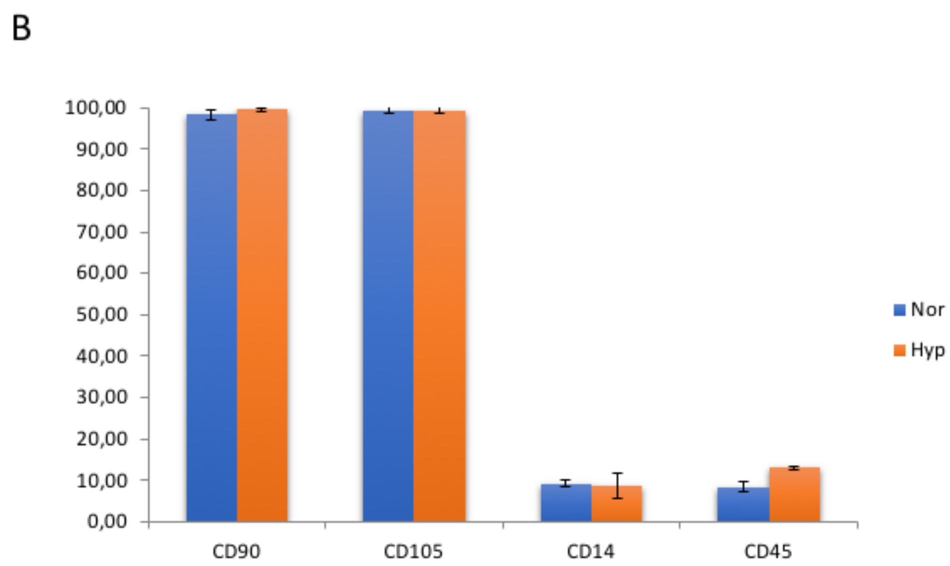

643

644 **Fig. 4.** Differentiation potential: Canine AT-MSCs cultured under adipogenic (A, D), 645 chondrogenic (B, E) and osteogenic (C, F) medium in normoxic and hypoxic conditions 646 respectively. G-L: Stained cells cultured in control medium. Magnification: 20X.

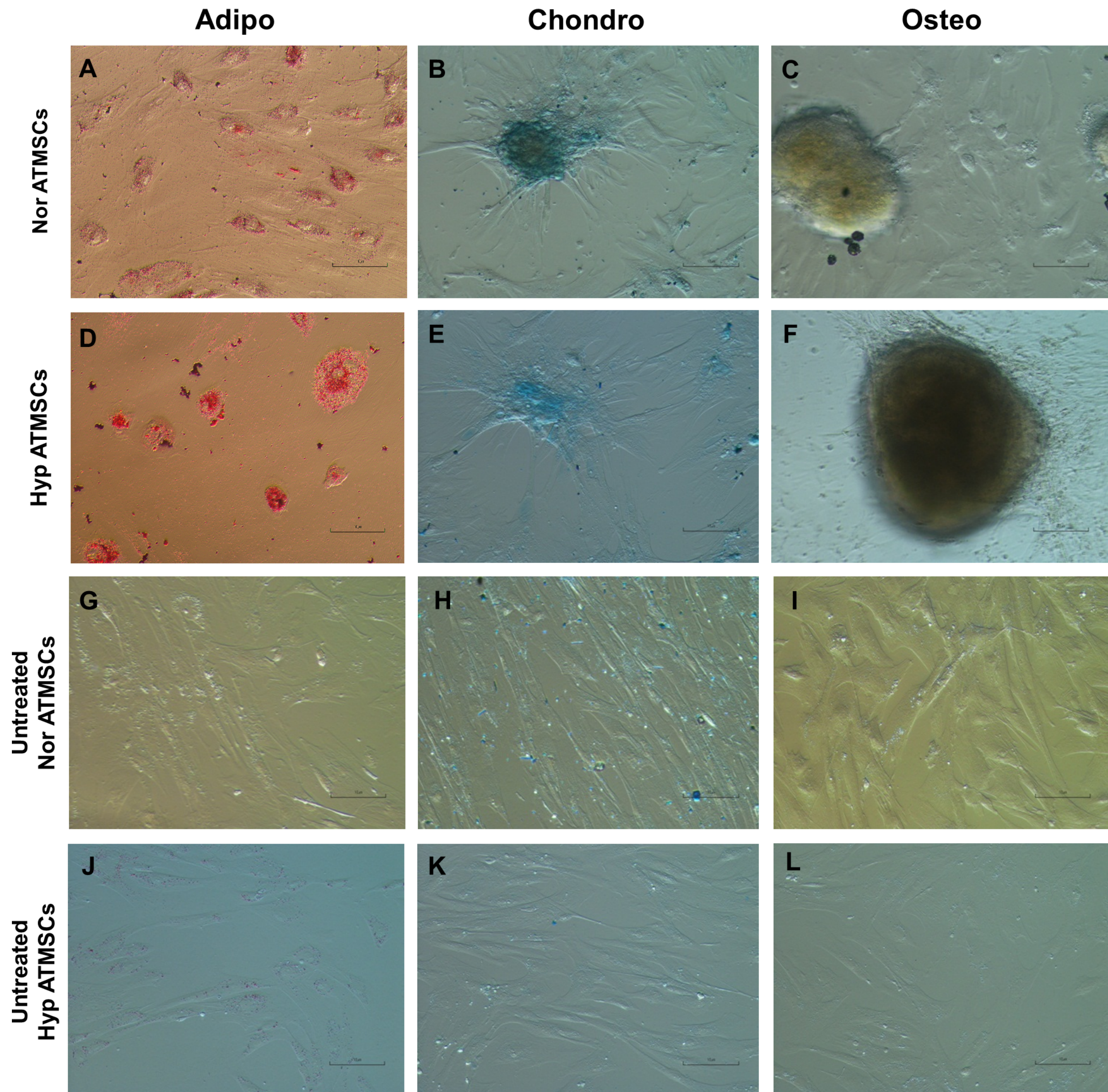

647

648 **Fig. 5**. Nor-AT-MSCs at TEM. **A.** At low magnification a single euchromatic irregular 649 nucleus containing a prominent nucleolus can be seen. Scale bar, 5µm. **B.** Note the abundance 650 of elongated mitochondria (arrow) and the well developed Golgi apparatus (arrowheads). 651 Scale bar 1 µm. **C.** A group of endolysosomes with heterogeneous content can be observed 652 (arrows). Near them, a dilated RER cistern has been marked with an asterisk. Scale bar, 1µm.

653 **D.** A maturing MVB containing numerous endo-luminal vesicles. Scale bar, 500 nm. **E.**
654 Numerous vesicles of heterogeneous size can be observed in the extracellular space. Scale
655 bar, 1 μm. **F.** Large complex electron-lucent vesicles budding from the cell surface and
656 containing smaller vesicles. Scale bar, 2 μm.

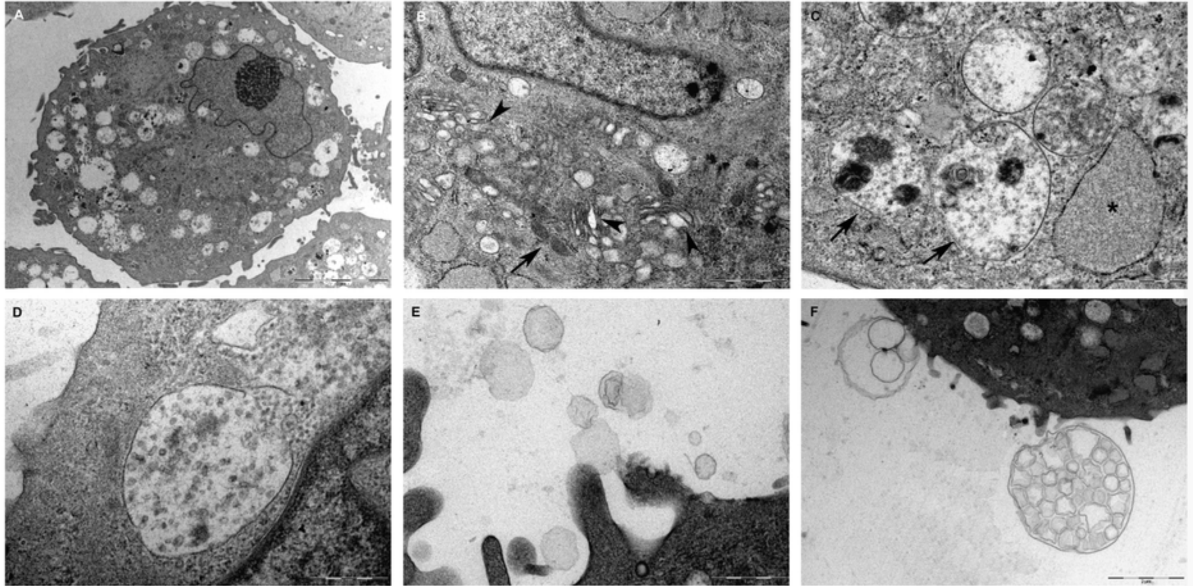

657

658 **Fig. 6.** Hyp-AT-MSCs at TEM. **A.** Low magnification image showing a single euchromatic
659 nucleus (arrow) and cytoplasm containing a prominent RER with dilated cisternae
660 (arrowheads). Note the irregular cell profile determined by the presence of cytoplasmic
661 pseudopodial evaginations. Scale bar, 10 μm. **B**. Cell cytoplasm with abundant mytochondria
662 (arrows), dilated RER and numerous MVB and endolysosomes (asterisks). Scale bar, 2 μm.
663 **C.** Golgi apparatus is wide and well developed and is characterized by flattened cisternae,
664 transport vesicles, and large vacuoles, often filled with fine granular material. Scale bar, 500
665 nm. **D**. The image shows the presence of vesicles of heterogeneous dimensions located in the
666 extracellular space. Scale bar, 2 μm. **E, F**. Note the presence of large vesicles shedding from
667 the cell surface and containing round-shaped smaller vesicles inside their lumen. Scale bar, 5
668 μm and 2 μm.

669

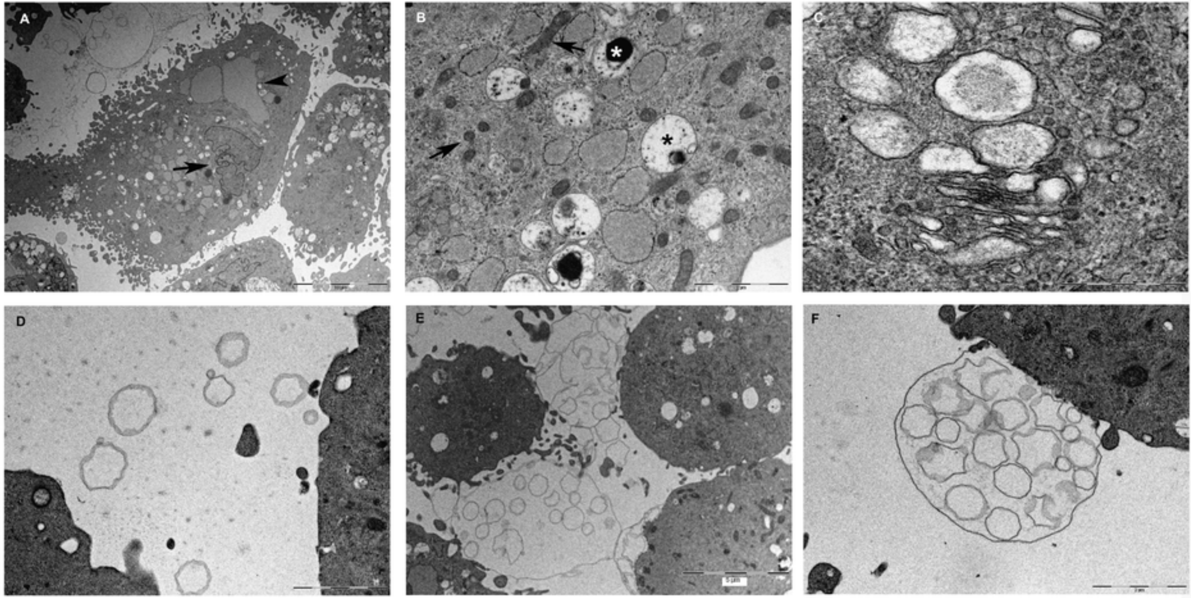

670

671 **Table 1**: Specific induction media compositions.

Adipogenic medium	Chondrogenic Medium	Osteogenic Medium
- DMEM/TCM199 - 10% FBS - 0.5 mM IBMX (removed after 3 days) - 1 μM DXM (removed after 6 days) - 10 μg/ml insulin - 0.1 mM indomethacin	- DMEM/TCM199 - 1% FBS - 6.25 μg/ml insulin - 50 nM AA2P - 0.1 μM DXM -10 ng/ml hTGF-β1	- DMEM/TCM199 - 10% FBS - 50 μM AA2P - 0.1 μM DXM - 10 mM BGP

672 IBMX: isobutylmethylxanthine, DXM: Dexamethasone, hTGF: human Transforming Growth

673 Factor, AA2P: Ascorbic Acid 2-Phosphate, BGP: Beta-Glycerophosphate

674

675 **Table 2**: Sequences of primers used for RT-PCR analysis

Gene	Primer sequences FW and RV	Amplicon (bp)	Reference
GAPDH	FW 5'- GGTCACCAGGGCTGCTTT -3' RV 5'- ATTTGATGTTGGCGGGAT -3'	209	(Jung et al. 2009)
CD44	FW 5'- GCCCTGAGCGTGGGCTTTGA -3' RV 5'-TCTGGCTGTAGCGGGTGCCA -3'	268	(Filioli Uranio et al. 2011)
CD34	FW 5'- GCCTGCTCAGTCTGCTGCCC-3' RV 5'- TGGTCCCAGGCGTTAGGGTGA -3'	255	(Filioli Uranio et al. 2011)
DLA-DRA1	FW 5'-CGCTCCAACCACACCCCGAA -3' RV 5'- GGCTGAGGGCAGGAAGGGGA-3'	246	(Filioli Uranio et al. 2011)
DLA-DQA1	FW 5'-GCACTGGGGCCTGGATGAGC -3' RV 5'-ACCTGAGCGCAGGCCTTGGA -3'	163	(Filioli Uranio et al. 2011)

676

677

678 **Table 3.** Primary antibodies and Isotype used for flow cytometry.

Markers	Ig
CD90 - PC5	IgG1
CD105 - PE	IgG2a
CD14 - PC5	IgG2a
CD45 - APC	IgG1
Isotype	
Isotype PC5	IgG2a
Isotype FITC	IgG1
Isotype PE	IgG1
Isotype APC	IgG1

679 Ig: immunoglobin

680